

THE XMM LARGE SCALE STRUCTURE SURVEY: SCIENTIFIC MOTIVATION AND FIRST OBSERVATIONS

M. Pierre¹, I. Valtchanov¹, and A. Refregier²

¹Service d'Astrophysique, CEA/Saclay, F-91191 Gif sur Yvette, France; mpierre, ivaltchanov@cea.fr

²Institute of Astronomy, Madingley Road, Cambridge CB3 0HA, UK; ar@ast.cam.ac.uk

ABSTRACT

Thanks to its unrivalled sensitivity and large field of view, XMM potentially occupies a leading position as a survey instrument. We present cosmological arguments in favour of a medium-sensitivity, large-scale structure survey with XMM, using galaxy clusters as tracers of the cosmic network. We show how this has motivated the definition of a concrete survey, the XMM Large-Scale Structure Survey (XMM-LSS), which will cover 64 square degrees with a sensitivity about 1000 times better than the median ROSAT All-Sky Survey. We present our predictions for cluster counts based on the Press-Schechter formalism and detailed X-ray image simulations, and show how they agree with the cluster statistics from recent ROSAT cluster surveys. We also present the extensive multi-wavelength follow-up associated with XMM-LSS, as well as the first observations from the programme.

Key words: Missions: XMM-Newton – surveys – multi-wavelength – clusters of galaxies – QSOs

1. INTRODUCTION

Ten years after the completion of the ROSAT All-Survey (RASS), XMM, although not initially designed for it, is in a position to open a new era for X-ray surveys. Its high sensitivity, good PSF and large field of view, indeed makes XMM a unique instrument for the study of extragalactic large scale structure (LSS). In this respect, two key points may be emphasized:

- Firstly, a high galactic latitude field observed with XMM is “clean” as it contains only two types of objects, namely QSOs (pointlike sources) and clusters (extended sources).
- Secondly, clusters more luminous than $L_{[2-10]} \geq 3 \cdot 10^{44} \text{ h}_{50}^{-2} \text{ erg/s}$ can be detected out to $z = 2$ as extended objects with a 10 ksec XMM exposure. With this exposure, XMM reaches a sensitivity of $\sim 10^{-14} \text{ erg/s/cm}^2$ in [0.5-2] keV for extended sources (cf Fig. 4). This is about 1000 and 10 times deeper than the REFLEX (Böhringer et al 2001) and NEP (Henry et al 2001) single area surveys respectively and provides a much better angular resolution. This makes XMM a powerful wide angle X-ray imager, with a sensitivity which will remain unrivalled in the coming decade. In particular, XMM is in a unique position

to study the evolution of the cosmic network traced by clusters and QSOs. In Section 2, we briefly review the cosmological implications of structure formation models. In Section 3, we show how these translate into the proposed XMM survey design. In Section 4, we discuss the cosmological constraints which can be derived with the XMM-LSS. We also compare our analytical predictions for the XMM-LSS cluster counts with current observations of cluster statistics. Section 5 describes the multi-wavelength follow-up associated with the XMM survey. Finally, the first images from the AO-1 observations are presented in Section 6.

2. COSMOLOGICAL CONTEXT

Compared to galaxies, clusters of galaxies - the most massive bound structures in the Universe - offer considerable advantages for LSS studies, both because they can provide complete samples of objects over a very large volume of space and because they are in some respects simpler to understand. The haloes of clusters can be traced by their X-ray emission (luminosity, size) while the theory describing their formation (biasing) and evolution from the initial fluctuations can be tested with numerical simulations. Such a level of understanding does not exist for galaxies and even less so for QSO formation. Studies of cluster LSS and cluster abundances are thus powerful tools to constrain cosmological parameters, independently of CMB and SNe studies. In addition, they can be used to test the validity of fundamental assumptions of the standard paradigm, such as the gravitational instability scenario. Given the capabilities of XMM and the fact that the previous cluster LSS survey (REFLEX, Böhringer et al 2001) was limited to $z \leq 0.3$, we have designed a project, the XMM-LSS, aiming at mapping the distribution of matter out to redshifts $\sim 1 - 2$ and the evolution of the cosmic network. The XMM observations constitute the core of the project, and are complemented by an extensive multi-wavelength follow-up programme to identify and study the astrophysical properties of the X-ray sources in detail.

3. SURVEY DESIGN

3.1. DEFINING THE SURVEY

The following theoretical and practical constraints have led to the current design of the XMM-LSS Survey :

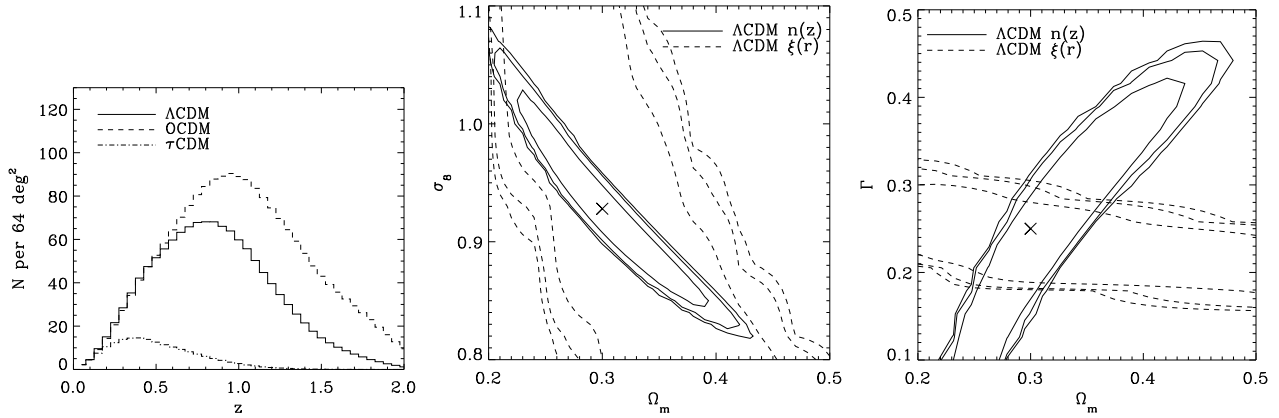


Figure 1. Cosmological constraints from the XMM-LSS (from Refregier et al (2001)). **Left:** The predicted XMM-LSS cluster redshift distribution for different cosmological models. The selection function for the XMM-LSS, generated from image simulations, was used to predict the observed counts. The currently favoured values of the cosmological parameters were used for each model. Note however that the resulting counts depend strongly on σ_8 , the normalisation of the matter fluctuations on $8 h^{-1}$ Mpc scale (see Fig. 7 of Refregier et al (2001)); **Centre:** Constraints upon the cosmological parameters Ω_m and σ_8 for a Λ CDM universe obtained from XMM-LSS cluster counts (solid lines) and correlation function (dashed lines). In each case, the 68%, 90% and 95% confidence level contours are shown along with the assumed model (cross). Cluster abundance data provides strong constraints upon the $\Omega_m - \sigma_8$ combination. **Right:** Constraints upon the cosmological parameters Γ (the shape of the matter power spectrum) and Ω_m for a Λ CDM universe (symbols defined as before). The correlation function is a powerful tool to constrain the shape of the initial spectrum. These calculations have been performed assuming that redshifts are available only over the $[0 < z < 1] \times [64 \text{ deg}^2]$ volume. Note that the detection of a Coma-type cluster within the XMM-LSS over the redshift range $1.5 < z < 2$ has a probability of $\sim 6.5 \times 10^{-7}$ in the current Λ CDM scenario. Therefore, any such discovery in the survey would put the currently favoured cosmological model in severe observational difficulty.

- Detect a significant fraction of the cluster population out to $z \sim 1$.
- Measure the cluster correlation function in two redshift bins between $0 < z < 1$, with a good level of accuracy (about 15% on the correlation length for both redshift intervals). This implies a minimum of about 400 clusters for each bin. The measurement of the evolution of the cluster correlation function is a fundamental test of structure formation models, but has never been done until now because of a lack of sufficiently wide and deep surveys.
- Probe a comoving length which is significantly larger than $100 h^{-1} \text{Mpc}$ at $z \sim 1$, the characteristic scale in the galaxy power spectrum of the local universe (e.g. Landy et al (1996)). This constrain corresponds to an opening survey angle of $\sim 10^\circ$ at $z = 1$ (i.e. $400 h^{-1} \text{Mpc}$)
- Find the best compromise between the two above constrains in order to minimise the necessary XMM observing time.
- Find an optimal survey location. An equatorial field is optimal, as ground-based follow-up resources from both hemispheres may be used. High galactic latitude and the absence of bright X-ray sources (e.g. nearby clusters) are also required. Moreover, the visibility of the field by XMM

must be $\geq 15\%$. Given this, only one area in the sky turned out to be favorable.

These different constraints led to the following lay-out: A 8×8 sq. deg. area paved with 10 ks XMM pointing separated by 20 arcmin (i.e. 9 pointings per sq.deg.). The field is centered around $\alpha = 2^{\text{h}}20^{\text{m}}$, $\delta = -5^\circ$ (at $b = -58^\circ$, with neutral hydrogen column $2 \times 10^{20} < N_H/\text{cm}^2 < 5 \times 10^{20}$). The resulting sensitivity is $\sim 3 \times 10^{-15}$ erg/s/cm 2 for pointlike sources in the $[0.5-2]$ keV band and of the order of $\sim 10^{-14}$ for extended sources. This area surrounds two deep XMM surveys based on guaranteed time: the XMM-SSC/Subaru Deep Survey (80 ks exposures in 1 deg^2) and the XMM Medium Deep survey (XMDS; 20 ks exposures in 2 deg^2), the latter being a collaboration between several instrumental teams: XMM-OM (Liège), XMM-EPIC (Milan-IFCTR), XMM-SSC (Saclay); MegaCam (Saclay, IAP); VIRMOS (LAM, IFCTR, OAB). The area overlap will greatly assist in quantifying the completeness of the survey.

3.2. THE XMM-LSS CONSORTIUM

The wide scope of the project has motivated the set-up of a large consortium to facilitate both the data reduction/management and the scientific analysis of the survey. The XMM-LSS Consortium comprises the following institutes: Saclay (Principal Investigator), Birmingham, Bristol, Copenhagen, Dublin, ESO/Santiago, Leiden, Liège, Marseille (LAM), Milan (AOB), Milan (IFCTR), Munich (MPA), Munich (MPE), Paris(IAP), Santiago (PUC).

4. CONSTRAINING COSMOLOGY

4.1. ANALYTICAL PREDICTIONS

We have studied quantitatively the prospects that the XMM-LSS cluster catalogue offers for measuring cosmological parameters (Refregier et al (2001)). We used the Press-Schechter (PS) formalism to predict the counts of clusters and their X-ray properties in several CDM models. We computed the detection efficiency of clusters, using realistic simulations of XMM images, and study how it differs from a conventional flux limit. We computed the expected correlation function of clusters using the extended halo model. Results are discussed in Fig. 1 and can be summarized as follows:

- The cluster counts set strong constraints on the value of the $\Omega_m - \sigma_8$ combination (the matter density and the amplitude of mass fluctuations on $8 h^{-1}$ Mpc scale). This combination will also provide a consistency check for the Λ CDM model, and a discrimination between this model and the OCDM model.
- The addition of the cluster 2-point correlation function provides a constrain on Γ , the shape of the initial density fluctuation power spectrum.
- With the current survey design, the *simultaneous* expected precision on Ω_m, σ_8 and Γ is about 15%, 10%, 35% respectively.

While these predictions are based on analytical calculations and image simulations, it is worth emphasizing that they agree with the latest measurements of XMM specifications and cluster statistics. Firstly, XMM has now proved to reach its nominal sensitivity in normal observing conditions. Secondly, we have used in our predictions, a value of $\sigma_8 = 0.93 \pm 0.07$ for $\Omega_m = 0.3$, as measured with the cluster temperature function (Eke et al (1996)). For the currently favoured Λ CDM model, this yields some 370 and 520 clusters detected in the $0 < z < 0.6$, $0.6 < z < 1$ intervals respectively, having a temperature greater than 2 keV. The present uncertainties on σ_8 globally result in a factor of 2 on our predicted cluster numbers (i.e. from 600 to 1200 clusters detections expected within $0 < z < 1$). The high sensitivity to σ_8 is not surprising, as it is precisely that which makes cluster counts a good measure of this parameter. This uncertainty can be reduced by analysing about 10 sq.deg. of the XMM-LSS, the minimum area required to improve upon the current mea-

surements of σ_8 in the presence of shot noise and cosmic variance. This has practical consequences for the number of optical spectroscopic nights needed to measure cluster redshifts. However, beyond the current nominal value of ~ 15 clusters per sq.deg, a random sampling of the cluster population would be sufficient to fulfill our cosmological goals.

4.2. COMPARISON WITH CURRENT OBSERVATIONS

To further validate our predictions, we have compared our analytical model with the current measurements of cluster statistics. For this purpose, we first considered the cluster luminosity function $F(L)$. Figures 2 and 3 show the measurement of $F(L)$ from the ROSAT Deep Cluster Survey (RDCS, Rosati et al (1998)) at $z = 0$ and $z = 0.8$. As can be seen on the figures, the measured luminosity function was shown not to evolve in this redshift interval. Note that, in Figure 3, the RDCS $F(L)$ was extrapolated to low luminosities ($L_{[0.5-2]} \simeq 1.5 \cdot 10^{43} h_{50}^{-2}$ erg/s (EdS) at $z = 0.8$) in order to match the XMM-LSS flux limit ($\sim 10^{-14}$ erg/s in [0.5-2] keV) which is about 3 times lower than that of RDCS ($L_{[0.5-2]} \simeq 4 \cdot 10^{43} h_{50}^{-2}$ erg/s (EdS) at $z = 0.8$, Rosati et al (1998)). We also calculated the analytical luminosity function using the mass function from the Press-Schechter formalism for haloes with $T > 1keV$, the $M - T$ relationship assuming virial equilibrium, and the $L - T$ relationship measured by Arnaud & Evrard (1999). As can be seen on Figures 2 and 3, the comparison with the observed luminosity function shows good agreement. Indeed, the agreement is better than a factor of 2 for bolometric luminosities lower than 10^{44} erg/s, which represent the bulk of our cluster population. As shown in Figures 2 and 3, the Sheth & Tormen (1999) formalism, which provides a better fit to N-body simulations than PS, further improves the match for high luminosity objects.

As a more practical test, we also compared our predicted cluster counts $N(z)$ with that obtained by a direct integration of the observed luminosity function. For the latter, we adopted the same flux limit as above (using redshifted Raymond-Smith spectra), and used the non evolving $L-T$ relationship from Arnaud & Evrard (1999). We also extrapolated $F(L)$ at high redshifts to lower luminosities (as described above) and extended the validity of the RDCS $F(L)$ from $z = 0.8$ to $z = 1$ (the minimum luminosity corresponding to our flux limit is $L_{[0.5-2]} \simeq 3 \cdot 10^{43} h_{50}^{-2}$ erg/s at $z = 1$). As shown in Figure 4, the two distributions are in good agreement. In the present calculation, we assumed that RDCS is not evolving (Rosati et al (1998)); there is however growing evidence that massive clusters are less numerous at high redshift (Henry 2001). This would improve further the agreement with our simulations. Consequently, our analytical model is consistent with the current measurements of cluster statistics, and thus provides secure predictions for the cluster counts in the XMM-LSS.

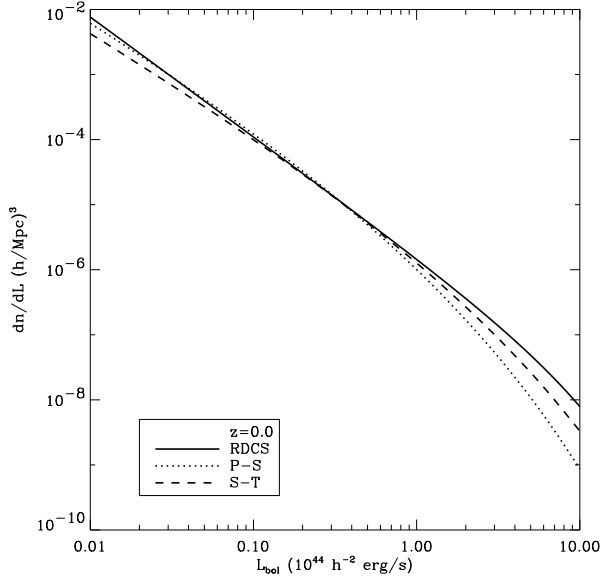


Figure 2. The cluster luminosity function at $z = 0$. Solid line: observed from RDCS. Dotted line: our predictions using the PS formalism. Dashed line: same, but using Sheth-Tormen formalism (Sheth & Tormen (1999)), which provides a better fit to N -body simulations.

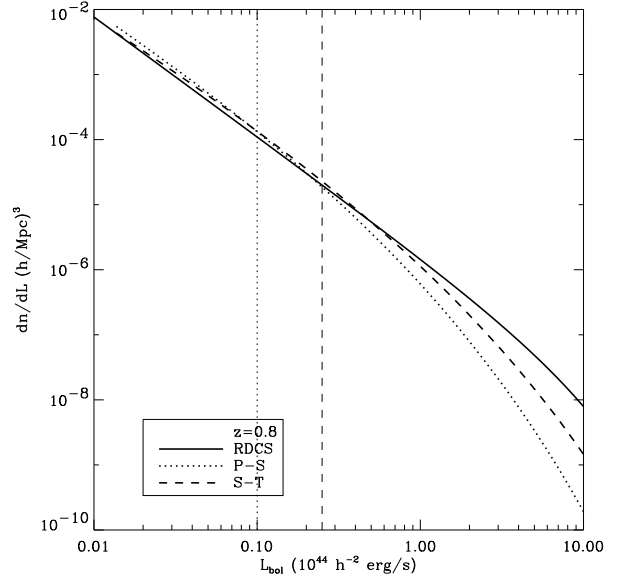


Figure 3. Same as Fig. 2, but for $z = 0.8$. Here the RDCS $F(L)$ has been extrapolated beyond $L_{bol} \simeq 2.5 \cdot 10^{43} \text{ erg/s}$ (Λ CDM), which corresponds to $L_{[0.5-2]} \simeq 4 \cdot 10^{43} h_{50}^{-2} \text{ erg/s}$ (EdS), the current limit of the RDCS at $z = 0.8$ (vertical dashed line). The vertical dotted line represents the XMM-LSS detection 90% limit for clusters at $z = 0.8$.

5. MULTI-WAVELENGTH FOLLOW-UP

Imaging: The imaging of the $8 \times 8 \text{ deg}^2$ XMM-LSS area is the priority target of the Canada-France-Hawaii Legacy Survey¹. MegaCam is a one degree field imager built by CEA to be installed at the new CFHT prime focus. It will come into operation by mid-2002. It will provide the deep high quality optical multi-color imaging counterpart of the X-ray sources ($u^*=25.5$, $g'=26.8$, $r'=26.0$, $i'=25.3$, $z'=24.3$) at a rate of $15 \text{ deg}^2/\text{yr}$ in at least three colours. In particular, an optical cluster catalogue is currently under construction using the CFH12K (and later MegaCam) observations using both spatial clustering analysis and multi-color matched filter techniques, in addition to photometric redshift estimates. Moreover, the MegaCam data will form the basis of a weak lensing analysis², whose cosmological constraints will be compared to that provided by the X-ray data on the same region. This will be the first, coherent study of LSS on such scales. R and z' imaging from CTIO are also being analyzed. Data pipelines and processing have been developed by the TERAPIX³ consortium; this will provide object catalogues and astrometric positions for the entire surveyed region. In addition, deep NIR VLT imaging (J, H, K) of $1 < z < 2$ cluster candidates found in in

the XMM-LSS will be performed as a confirmation prior to spectroscopy.

Spectroscopy: The standard spectroscopic follow-up is designed to perform redshift measurements for all identified $0 < z < 1$ X-ray clusters in Multi-Object-Spectroscopy mode, using the 4m and 8m telescopes to which the consortium has access. We plan to take 1 mask per cluster, randomly sampling the XMM AGN population at the same time, as well as the surrounding filamentary galaxy distribution connecting clusters. This mapping around $0 < z < 1$ clusters will have an important scientific potential for studies of galaxy environments and bias. We shall subsequently undertake programmes of advanced spectroscopy that will focus on individual objects, and include high resolution spectroscopy, the measurement of cluster velocity dispersions, QSO absorption line surveys, as well as NIR spectroscopy of our $z > 1$ cluster candidates.

Radio: In the radio waveband, the complete survey region is being mapped using the VLA at 74MHz and 325MHz. Radio coverage is not only particularly relevant for tracing merger events triggered by structure formation, but also as a useful indicator of galactic nuclear or star-formation activity.

Sunyaev-Zel'dovich: observations (S-Z) are also planned. Clusters in the XMM-LSS field will be targets of the prototype OCRA (One-Centimeter Radiometer Array) instrument from 2002. The full XMM-LSS field will be mapped by the complete OCRA, and will be an early target of the Array for Microwave Background Anisotropy (AMiBA)

¹ <http://cdsweb.u-strasbg.fr:2001/Instruments/Imaging/Megacam/MSWG/forum.html>

² <http://www.iap.fr/LaboEtActivites/ThemesRecherche/Lentilles/LentillesTop.html>

³ <http://terapix.iap.fr>

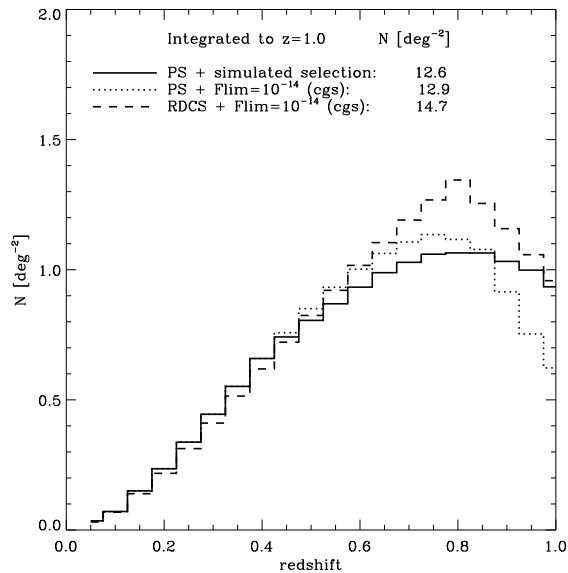


Figure 4. Comparison of analytical predictions for the cluster number count to that derived from a direct integration of the observed luminosity function. Solid line : Refregier et al (2001) predictions using PS formalism and detailed image simulations. Dotted line : same, but using a flux limit of 10^{-14} erg/s/cm² in [0.5-2] keV. Dashed line: predicted $N(z)$ using the RDCS luminosity function $F(L)$ extrapolated down to $L_{0.5-2} \simeq 1.6 \cdot 10^{43} h_{50}^{-2}$ erg/s (EdS) in order to reach the XMM-LSS flux limit of $\sim 10^{-14}$ erg/s/cm² out to $z = 0.8$; also $F(L)$ is assumed not to evolve out to $z = 1$. At z close to 1, Refregier et al (2001) predict less clusters than expected from $F(L)$ alone, since they take evolution into account. Λ CDM cosmology was assumed in all cases.

after 2004 (Liang (2001)). This will enable a statistical analysis of the physics of the ICM as a function of redshift. In the long term, these observations will also provide invaluable information on the low density structures such as cluster outskirts and groups, and their connections to supercluster filaments. These measurements are complementary to the X-ray and weak lensing surveys, connecting the mass distribution of clusters to the structure of the hot gas they contain. The three data sets together will also provide a direct and independent check of the extragalactic distance scale.

Infrared: In the infrared, the SWIRE⁴ SIRTf Legacy Programme will cover 10 deg² of the XMM-LSS in 7 wavebands from 4 to 160 mm. The estimated IR source numbers in this area are around 20000/900/250 and 700/50/500 for starbursts/spiral-irregular/AGN in the $0 < z < 1$ and $1 < z < 2$ redshift intervals, respectively. This represents a unique X-ray/IR combination in depth and scales to be probed. The coordinated SWIRE/XMM-LSS observa-

tions will clarify an important aspect of environmental studies, namely how star formation in cluster galaxies depends on the distance to the cluster centre, on the strength of the gravitational potential, and on the density of the ICM. In this respect the XMM-LSS represents the optimum SWIRE field, where galaxy environment, deep NIR imaging and optical spectroscopic properties will be the main parameters in modelling the MIR/FIR activity. Here also, the location of IR AGNs within the cosmic web will help establish their nature. The FIR/X/optical/radio association will also provide unique insights into the physics of heavily obscured objects, as well as the first coherent study of biasing mechanisms as a function of scale and cosmic time, for X-ray hot (XMM), dark (weak lensing), luminous galactic (optical/NIR) and obscured (SWIRE) material.

In summary, the XMM-LSS multi- λ data set will offer the first evolving view of structure formation from supercluster to galaxy scales. Its comprehensive approach constitutes a decisive new step in the synergy between space and ground-based observatory resources and therefore a building block of the forthcoming Virtual Observatory.

6. FIRST XMM OBSERVATIONS

For the XMM AO-1, about 700 ks have been allocated to the project (GT and GO time) corresponding to some 50 pointings. First pointings were performed in July 2001. Some of them are presented on Fig. 5. Our first analysis of the data confirms our predictions for the XMM sensitivity with 20 ks. Fig. 6 shows two examples of extended sources found in the preliminary analysis: one compact group and one distant cluster candidate. The overlays give a good impression of the mean source density and emphasize the need for multi-color ground-based imaging in the process of source identification.

7. MORE INFORMATION

More information is available on the XMM-LSS web page: http://vela.astro.ulg.ac.be/themes/spatial/xmm/LSS/index_e.html

REFERENCES

- Arnaud, M. & Evrard, A., 1999, MNRAS, 305, 631
 Böhringer H., Schuecker P., Guzzo L., Collins C. A., Voges W., Schindler S., Neumann D. M., Cruddace R. G., De Grandi S., Chincarini G., Edge A. C., MacGillivray H. T., Shaver P., 2001, A&A 369, 826
 Eke, V.R., Cole, S., & Frenk, C.S., 1996, MNRAS, 282, 263
 Henry J. P., Gioia I.M., Mullis C.R., Voges W., Briel U.G., Böhringer H., 2001, ApJ Let 553, L109
 Henry J. P., 2001, astro-ph/0109498
 Landy S.D. et al., 1996, ApJ 456, L1
 Liang H., 2001, astro-ph/0110518
 Refregier A., Valtchanov I., Pierre M., 2001, submitted to A&A, astro-ph/0109529.

⁴ <http://www.ipac.caltech.edu/SWIRE>

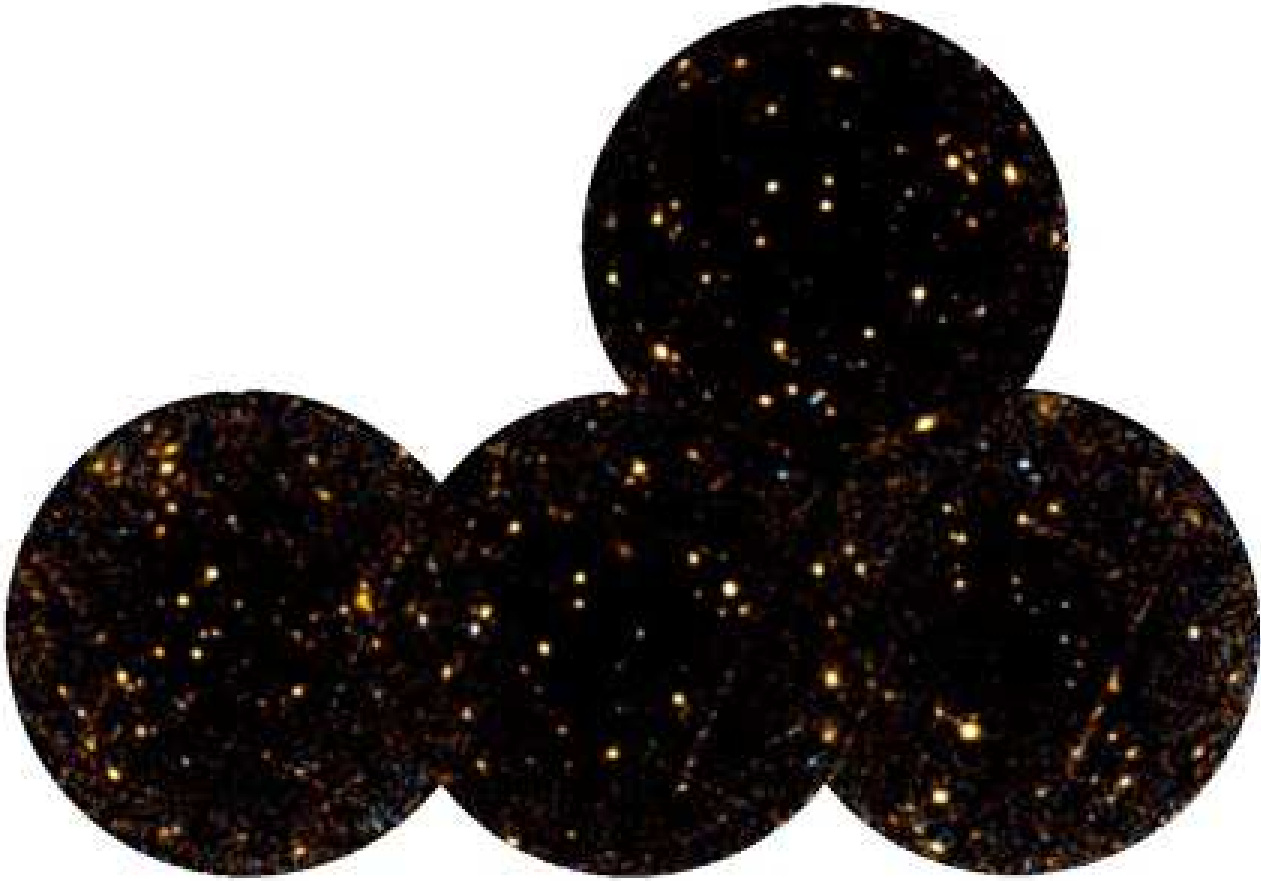


Figure 5. First XMM pointings of the survey obtained during the Guaranteed Time part of the programme led by the Liège/Milano/Saclay groups. This preliminary mosaic in true X-ray colours is a fraction of the central deeper 2 sq.deg. area; red: soft sources (< 2 keV), blue: hard sources (> 2 keV). The individual images have a diameter of 25 arcmin and the exposure time is 20 ks on each field. The source density is found to be ~ 600 / sq.deg. in the [0.5-2] keV band (Valtchanov et al 2002, in preparation). It is interesting to note that this field is devoid of sources in the ROSAT All-Sky Survey.

Rosati P., della Ceca R., Norman C., Giacconi R., 1998, ApJ
Let 492, 21L
Sheth R. K. Tormen G., 1999, MNRAS 308, 119

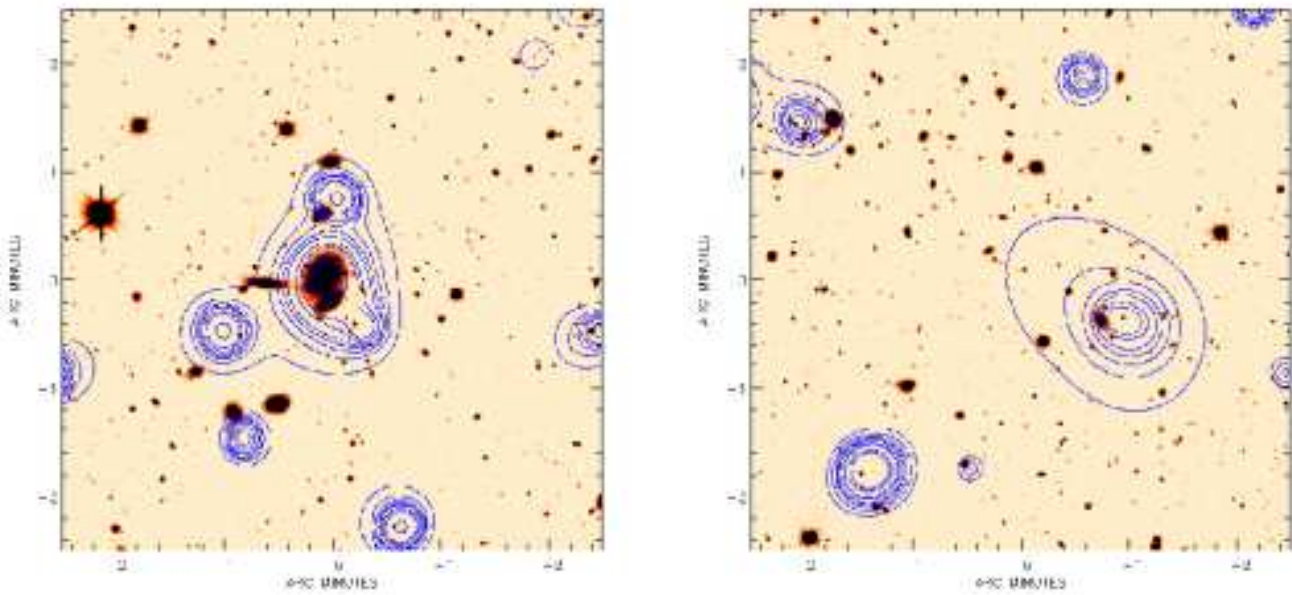


Figure 6. Overlaid on a deep CFH12K I image (VIRMOS Deep Survey, by Le Fèvre et al.), the XMM contours are shown in the [0.5-2] keV band (after wavelet filtering). **Left:** The central source is very soft and found to be associated with a compact group in the optical. This object was not known prior to our observation, although already flagged as a 2MASS source. Several other pointlike sources are conspicuous on the image, but few of them have an obvious optical identification. **Right:** The clearly extended source toward the image center has no obvious optical counterpart and, therefore, is an interesting distant cluster candidate. Such a situation enlightens the need for deep NIR photometry in order to confirm the existence of $z > 1$ clusters, to provide photometric redshifts and, eventually, galaxy targets for a spectroscopic measurement